CHEMISTRY OF MATERIALS

COMMUNICATION

pubs.acs.org/cm

Graphene Decorated with PtAu Alloy Nanoparticles: Facile Synthesis and Promising Application for Formic Acid Oxidation

Sheng Zhang,[†,‡] Yuyan Shao,[‡] Hong-gang Liao,[‡] Jun Liu,[‡] Ilhan A. Aksay,[§] Geping Yin,[*,†] and Yuehe Lin[*,‡]

[†]School of Chemical Engineering & Technology, Harbin Institute of Technology, Harbin 150001, China

[‡]Pacific Northwest National Laboratory, Richland, Washington 99352, United States

[§]Department of Chemical and Biological Engineering, Princeton University, Princeton, New Jersey 08544, United States

Supporting Information

KEYWORDS: carbon materials, catalysis and catalysts, electrochemistry

Bimetallic nanoparticles (NPs) have recently received much attention as electrocatalysts.[1−3] Pt is the most effective catalyst for fuel cells: it facilitates oxygen reduction at a cathode[4] and hydrogen (or small organic molecules) oxidation at an anode.[5] Au is one of only two transition metals more electronegative than Pt, so the incorporation of Au has unique effects on Pt NPs.[1] Therefore, bimetallic PtAu NPs are of fundamental interest and importance as fuel cell electrocatalysts, especially for formic acid oxidation.[6,7] However, due to the miscibility gap between Pt and Au, the synthesis of the PtAu alloy sample is an open challenge.[8−10] Thus, it is necessary to develop an effective approach to synthesize PtAu alloy NPs.

To maximize the electrocatalytic activity of PtAu NPs, a suitable carbon support is required to disperse these NPs. Conventional carbon supports for electrocatalysts include XC-72 carbon black (CB) and carbon nanotubes. Recently, graphene, a single-atom-thick sheet of hexagonally arrayed sp^2-bonded carbon atoms, has been extensively studied in physics, chemistry, and materials fields.[11,12] Due to its huge surface area (~2600 m^2 g^{-1}), high electrical conductivity (10^5−10^6 S m^{-1}), and excellent catalytic activity,[13,14] graphene has been considered as a promising candidate as a new 2D support to load Pt, Pd, and Au NPs for applications in fuel cells and catalysis.[15−19] However, it is difficult to uniformly load metal NPs on graphene due to its hydrophobic properties.[18]

Here, we present a facile approach to synthesize PtAu alloy NPs uniformly dispersed on graphene (PtAu/graphene). The key is the introduction of poly(diallyldimethylammonium chloride) (PDDA), which not only acts as "nanoreactors" for the preparation of PtAu alloy NPs[20] but also facilitates the uniform loading of PtAu NPs on graphene. More importantly, PtAu/graphene hybrids exhibit high electrocatalytic activity toward formic acid oxidation. Graphene used here was produced by a process described elsewhere and is intrinsically functionalized with hydroxy, epoxy, carboxls, and lattice defect sites.[21,22] The details for the synthesis of PtAu/graphene nanocomposites (Pt:Au = 1:1) can be seen in Supporting Information. For comparison, PtAu/CB was prepared with the same method.

The morphological structure, the particle size, and the dispersion of PtAu/graphene and PtAu/CB were examined by transmission electron microscopy (TEM). Figure 1a displays the as-prepared graphene as a crumpled nanosheet. Typical TEM images of PtAu/graphene with different magnifications (Figure 1b,c) show that PtAu NPs with a volume/area averaged diameter[20] of 3.3 ± 0.2 nm (calculated from the histogram of particle size distribution as shown in Supporting Information Figure S1) are uniformly dispersed on graphene nanosheets. The particle size (3.2 ± 0.2 nm) and the dispersion of PtAu NPs on CB (Figure 1d) are similar to that of PtAu/graphene.

To analyze the average particle size and study the Pt−Au alloy effect, PtAu/graphene and PtAu/CB were characterized by X-ray diffraction (Figure 2). The peaks at 38.86°, 45.03°, 65.95°, and 79.14° can be assigned to PtAu(111), -(200), -(220), and -(311), clearly demonstrating that PtAu NPs have a face-centered cubic (fcc) structure.[6] The (111) peak of PtAu is shifted to a lower angle by about 0.90°, compared with that of pure Pt (JCPDS 04-0802),[20] which indicates the higher d_{111} of PtAu (2.321 Å) than that of pure Pt (2.267 Å).[23] The lattice constant for the PtAu phase is a = 4.0199 Å, which is larger than that of pure Pt (a = 3.9231 Å) but smaller than that of pure Au (a = 4.0786 Å). This result confirms the PtAu alloy formation in the presence of PDDA.[6,9] In addition, the average particle size of PtAu alloy NPs calculated using the Scherrer equation from the peak (220)[24] is 3.1 nm, which is consistent with the TEM results.

PDDA is a cationic polyelectrolyte[25] and usually used to stabilize metal nanoparticles.[20] To the best of our knowledge, this is the first time that PDDA is employed to mediate the synthesis of PtAu alloy NPs. Compared with conventional methods (PtAu alloy nanoparticles prepared in the presence of sodium citrate had ~5 nm particle size and obvious aggregation on carbon support),[10,23] herein the PDDA-mediated PtAu alloy NPs exhibit smaller particle size and more uniform distribution. The reason is as follows. Once PDDA is added, Cl^- ions in PDDA rapidly exchange with $PtCl_6^{2-}$ and $AuCl_4^-$ ions,[26] which are confined within the "nanoreactors" formed by long chains of PDDA due to the electrostatic interaction,[20] and are rapidly reduced by $NaBH_4$ to form PtAu alloy. During the formation of PtAu alloy NPs, the electrostatic replusion between positively

Received: June 17, 2010
Revised: December 19, 2010
Published: January 11, 2011

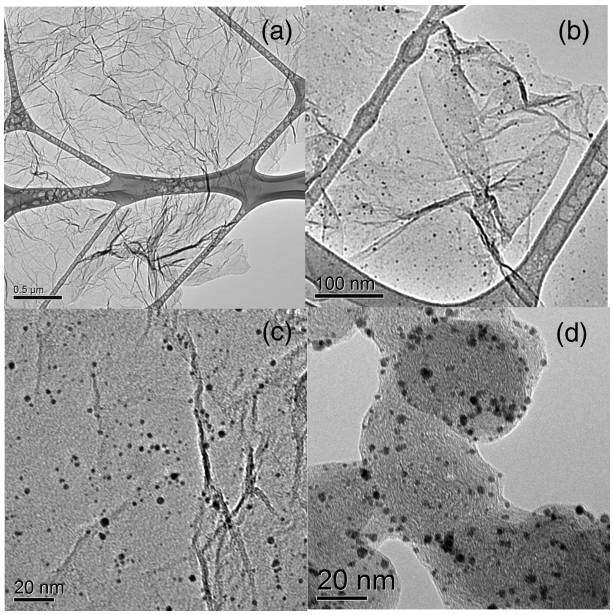

Figure 1. TEM images of graphene nanosheets (a), PtAu/graphene (b, c), and PtAu/CB (d).

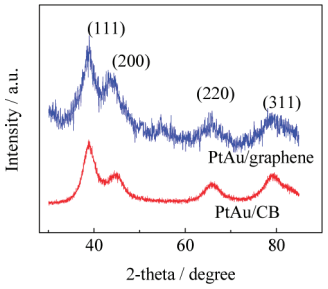

Figure 2. XRD patterns of PtAu/graphene and PtAu/CB.

charged functional groups in PDDA prevents PtAu NPs from aggregating, and long chains of PDDA also provide steric stabilization for these NPs.[25,27] Therefore, the presence of PDDA makes the small-sized PtAu alloy NPs stable in the solution.

Another important role of PDDA is to facilitate the uniform loading of PtAu NPs on graphene nanosheets. It is well-understood that hydrophobic graphene tends to form agglomerates due to van der Waals interaction, which makes the dispersion of nanoparticles on graphene difficult.[17] In this study, PDDA adsorbs on the surface of graphene nanosheets via $\pi-\pi$ interactions and prevents graphene nanosheets from aggregating together (shown in Supporting Information Figure S2), which can be attributed to the thermodynamic preference of graphene−PDDA interactions with respect to graphene−water interactions.[28] Further, as mentioned above, PtAu alloy NPs are confined within the long chains of PDDA, which spontaneously adsorbs on the surface of graphene. Therefore, PtAu alloy NPs exhibit high dispersion on the surface of graphene nanosheets.

The electrocatalytic capability of PtAu/graphene was evaluated in the solution of 0.5 M H_2SO_4 + 0.5 M HCOOH. Commercial Etek-Pt/C (Pt mass loading: 20%) and PtAu/CB were tested for comparison. The PtAu mass loadings evaluated by thermogravimetry analysis shown in Supporting Information Figure S3 are 18.2% and 18.7% for PtAu/graphene and PtAu/CB, respectively. As displayed in Figure 3a, PtAu/graphene and PtAu/CB exhibit much lower onset potential of formic acid oxidation than commercial Etek-Pt/C catalyst: 170 mV vs 300 mV. Moreover, the P_I peak current density on PtAu/graphene (2.310 A mg^{-1} Pt) and PtAu/CB (1.682 A mg^{-1} Pt) is much higher than that on Etek-Pt/C (0.182 A mg^{-1} Pt), although Etek-Pt/C catalyst has smaller Pt particle size (2.9 ± 0.2 nm, shown in Supporting Information Figure S1). These results indicate that PtAu/graphene and PtAu/CB have higher electrocatalytic activity toward HCOOH oxidation than Etek-Pt/C,[3,6] which can be assigned to the "ensemble effect" of Pt sites: the noncontinuous Pt sites formed in PtAu alloy NPs favor the direct oxidation process of formic acid.[4,6,7]

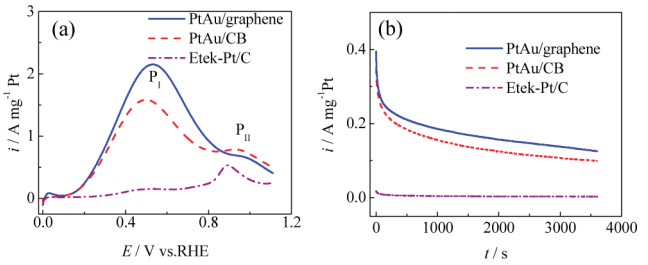

Figure 3. Formic acid oxidation (a) at the scan rate of 50 mV s^{-1} and amperometric $i-t$ curves (b) at a fixed potential of 0.3 V on PtAu/graphene, PtAu/XC-72, and commercial Etek-Pt/C in N_2-saturated 0.5 M H_2SO_4 + 0.5 M HCOOH.

It is worth noticing that PtAu/graphene exhibits 37% higher activity than PtAu/CB. Since PtAu NPs were prepared with the same method which have similar particle size/distribution and crystallinity in these two catalysts, the only difference lies in the carbon supports. In Figure 3a, the P_I peak is related to dehydrogenation reaction ($HCOOH \rightarrow CO_2 + 2H^+ + 2e^-$), while the P_{II} peak is ascribed to the dehydration reaction ($HCOOH \rightarrow CO_{ads} + H_2O \rightarrow CO_2 + 2H^+ + 2e^-$).[10,29] As shown in Figure 3a, the intensity of peak P_{II} on PtAu/graphene is lower than that on PtAu/CB, which indicates that less CO is generated on PtAu/graphene. So the presence of graphene in PtAu/graphene suppresses the formation of poisoning intermediate CO_{ads} during the formic acid oxidation. Sutter et al. have confirmed that the strong electronic interaction exists between graphene and metal NPs, which can affect chemical reaction parameters on the surface of metal NPs, such as adsorption energies.[30] Yoo et al. have reported that the CO adsorption rate on Pt NPs depends on carbon support: Pt/graphene has a much smaller CO adsorption rate than Pt/XC-72.[15] Therefore, the higher electrocatalytic activity of PtAu/graphene can be attributed to the strong electronic interaction between graphene and PtAu alloy NPs, which suppresses the poisoning CO_{ads} formation and facilitates the direct oxidation process of formic acid on the PtAu surface.

The catalytic stability of PtAu/graphene, PtAu/CB, and Etek-Pt/C was examined by an amperometric method. Figure 3b shows the amperometric $i-t$ curves of these three samples in N_2-saturated 0.5 M H_2SO_4 + 0.5 M HCOOH at 0.3 V, which is close to the anodic working potential in direct formic acid fuel cells (DFAFC).[31] The current density at 3600 s on PtAu/graphene is 0.120 A mg^{-1}, much higher than that on PtAu/CB (0.091 A mg^{-1}) and Etek-Pt/C (0.004 A mg^{-1}), which indicates that PtAu/graphene has the highest catalytic stability toward formic acid

dx.doi.org/10.1021/cm101568z |*Chem. Mater.* 2011, 23, 1079–1081

oxidation.[32,33] This result, combined with cyclic voltammetry (CV) measurements above, further confirms the superior catalytic activity and stability of PtAu/graphene toward HCOOH oxidation.

In summary, PtAu alloy NPs on graphene were prepared with a uniform dispersion via a polyelectrolyte-assisted process. PtAu/graphene exhibited highly electrocatalytic activity and stability for formic acid oxidation. The finding is of significance for the application of graphene because polyelectrolyte can faciliate the uniform disperson of metal NPs on graphene, which has been demonstrated as a promising anode electrocatalyst of direct formic acid fuel cells. Moreover, this facile preparation method can be readily extended to the synthesis of other alloy NPs.

■ ASSOCIATED CONTENT

Supporting Information. Experimental details, digital photos of water dispersions of graphene without and with PDDA, and thermogravimetry analysis (TGA) data. (PDF). This material is available free of charge via the Internet at http://pubs.acs.org.

■ ACKNOWLEDGMENT

This work was done at the Pacific Northwest National Laboratory (PNNL) and was supported by a LDRD program. The characterization was performed using EMSL, a national scientific user facility sponsored by the DOE's Office of Biological and Environmental Research and located at PNNL. PNNL is operated for the DOE by Battelle under Contract DE-AC05-76RL01830. S.Z. acknowledges a fellowship from the China Scholarship Council and PNNL to perform this work at PNNL. We acknowledge Dr. C. M. Wang for TEM characterization. G.Y. acknowledges the support from the Natural Science Foundation of China (No. 50872027). I.A.A. acknowledges support from ARRA/AFOSR under Grant No. FA9550-09-1-0523.

■ REFERENCES

(1) Zhang, J.; Sasaki, K.; Sutter, E.; Adzic, R. R. *Science* **2007**, *315*, 220.
(2) Rice, C.; Ha, S.; Masel, R. I.; Wieckowski, A. *J. Power Sources* **2003**, *115*, 229.
(3) Zhang, S.; Shao, Y. Y.; Yin, G. P.; Lin, Y. H. *Angew. Chem., Int. Ed.* **2010**, *49*, 2211.
(4) Mayrhofer, K. J. J.; Blizanac, B. B.; Arenz, M.; Stamenkovic, V. R.; Ross, P. N.; Markovic, N. M. *J. Phys. Chem. B* **2005**, *109*, 14433.
(5) Tian, N.; Zhou, Z. Y.; Sun, S. G.; Ding, Y.; Wang, Z. L. *Science* **2007**, *316*, 732.
(6) Xu, J. B.; Zhao, T. S.; Liang, Z. X.; Zhu, L. D. *Chem. Mater.* **2008**, *20*, 1688.
(7) Kristian, N.; Yan, Y. S.; Wang, X. *Chem. Commun.* **2008**, 353.
(8) Schrinner, M.; Proch, S.; Mei, Y.; Kempe, R.; Miyajima, N.; Ballauff, M. *Adv. Mater.* **2008**, *20*, 1928.
(9) Luo, J.; Maye, M. M.; Petkov, V.; Kariuki, N. N.; Wang, L. Y.; Njoki, P.; Mott, D.; Lin, Y.; Zhong, C. J. *Chem. Mater.* **2005**, *17*, 3086.
(10) Zhang, S.; Shao, Y. Y.; Yin, G. P.; Lin, Y. H. *J. Power Sources* **2010**, *195*, 1103.
(11) Wang, Y.; Shao, Y. Y.; Matson, D. W.; Li, J. H.; Lin, Y. H. *ACS Nano* **2010**, *4*, 1790.
(12) Shao, Y. Y.; Wang, J.; Engelhard, M.; Wang, C. M.; Lin, Y. H. *J. Mater. Chem.* **2010**, *20*, 743.
(13) Seger, B.; Kamat, P. V. *J. Phys. Chem. C* **2009**, *113*, 7990.
(14) Shao, Y. Y.; Zhang, S.; Engelhard, M. H.; Li, G. S.; Shao, G. C.; Wang, Y.; Liu, J.; Aksay, I. A.; Lin, Y. H. *J. Mater. Chem.* **2010**, *20*, 7491.
(15) Yoo, E.; Okata, T.; Akita, T.; Kohyama, M.; Nakamura, J.; Honma, I. *Nano Lett.* **2009**, *9*, 2255.
(16) Scheuermann, G. M.; Rumi, L.; Steurer, P.; Bannwarth, W.; Mulhaupt, R. *J. Am. Chem. Soc.* **2009**, *131*, 8262.
(17) Guo, S. J.; Dong, S. J.; Wang, E. K. *ACS Nano* **2010**, *4*, 547.
(18) Xu, C.; Wang, X.; Zhu, J. W. *J. Phys. Chem. C* **2008**, *112*, 19841.
(19) Si, Y. C.; Samulski, E. T. *Chem. Mater.* **2008**, *20*, 6792.
(20) Zhang, S.; Shao, Y. Y.; Yin, G. P.; Lin, Y. H. *J. Mater. Chem.* **2009**, *19*, 7995.
(21) McAllister, M. J.; Li, J. L.; Adamson, D. H.; Schniepp, H. C.; Abdala, A. A.; Liu, J.; Herrera-Alonso, M.; Milius, D. L.; Car, R.; Prud'homme, R. K.; Aksay, I. A. *Chem. Mater.* **2007**, *19*, 4396.
(22) Schniepp, H. C.; Li, J. L.; McAllister, M. J.; Sai, H.; Herrera-Alonso, M.; Adamson, D. H.; Prud'homme, R. K.; Car, R.; Saville, D. A.; Aksay, I. A. *J. Phys. Chem. B* **2006**, *110*, 8535.
(23) Park, I. S.; Lee, K. S.; Choi, J. H.; Park, H. Y.; Sung, Y. E. *J. Phys. Chem. C* **2007**, *111*, 19126.
(24) Zhang, S.; Shao, Y. Y.; Yin, G. P.; Lin, Y. H. *J. Mater. Chem.* **2010**, *20*, 2826.
(25) Pan, M.; Tang, H. L.; Jiang, S. P.; Liu, Z. C. *J. Electrochem. Soc.* **2005**, *152*, A1081.
(26) Sharma, G.; Ballauff, M. *Macromol. Rapid Commun.* **2004**, *25*, 547.
(27) Roucoux, A.; Schulz, J.; Patin, H. *Chem. Rev.* **2002**, *102*, 3757.
(28) Yang, D. Q.; Rochette, J. F.; Sacher, E. *J. Phys. Chem. B* **2005**, *109*, 4481.
(29) Zhou, X. C.; Xing, W.; Liu, C. P.; Lu, T. H. *Electrochem. Commun.* **2007**, *9*, 1469.
(30) Sutter, P.; Sadowski, J. T.; Sutter, E. A. *J. Am. Chem. Soc.* **2010**, *132*, 8175.
(31) Yu, X. W.; Pickup, P. G. *J. Power Sources* **2008**, *182*, 124.
(32) Wang, J. J.; Chen, Y. G.; Liu, H.; Li, R. Y.; Sun, X. L. *Electrochem. Commun.* **2010**, *12*, 219.
(33) Peng, Z.; Yang, H. *Nano Res.* **2009**, *2*, 406.